Erosion by flowing Martian lava: New insights for Hecates Tholus from Mars Express and MER data

David A. Williams and Ronald Greeley
Department of Geological Sciences, Arizona State University, Tempe, Arizona, USA

Ernst Hauber and Klaus Gwinner
Deutsches Zentrum für Luft- und Raumfahrt, Berlin, Germany

Gerhard Neukum
Institute of Geological Sciences, Freie Universität, Berlin, Germany

Received 4 November 2004; revised 7 March 2005; accepted 31 March 2005; published 19 May 2005.

[1] We have used new compositional information on Martian basaltic rocks from the Mars Exploration Rover Spirit and data from new stereo imaging by the High Resolution Stereo Camera (HRSC) on the Mars Express orbiter to constrain an existing analytical-numerical computer model to assess the potential of Martian lavas to form lava channels by erosion of substrate. The basaltic rocks studied in Gusev crater by Spirit have compositions consistent with lavas of higher liquidus temperature and lower dynamic viscosity than terrestrial tholeiitic basalts, suggesting that they had a greater potential for turbulent flow and erosion of substrate during flow emplacement than terrestrial basalts, more similar to lunar mare basalts. We modeled a specific case to determine whether these lavas could have formed part of a >66 km long channel on the Martian shield volcano Hecates Tholus. This channel formed on relatively steep slopes ($\sim$2–8°), based on measurements from the HRSC Digital Terrain Model. Our results suggest that erosion rates were of the order of tens to hundreds of centimeters/day, depending on flow rate and ice content of the substrate. Eruption durations required to erode the Hecates channel ($\sim$100–30 m deep over the first $\sim$20 km, depth decreasing downstream) range from weeks to months, which are consistent with the known eruption durations of terrestrial basaltic lavas and the previous modeling of Wilson and Mouginis-Mark (2004). Any Hecates lava channels formed from erosion by lava could have served as conduits for later fluvial activity, as recently described by Fassett and Head (2004, 2005).

Citation: Williams, D. A., R. Greeley, E. Hauber, K. Gwinner, and G. Neukum (2005), Erosion by flowing Martian lava: New insights for Hecates Tholus from Mars Express and MER data, *J. Geophys. Res.*, *110*, E05006, doi:10.1029/2004JE002377.

1. Introduction

[2] Since the discovery of sinuous rilles (channels) on the Moon [*Neison*, 1876; *Pickering*, 1903], planetary geologists have speculated about the genesis of lava channels on the terrestrial planets and satellites. Some of these features on the Moon and Mars resemble collapsed lava tubes on Earth [*Greeley*, 1971a, 1971b], whereas others have the morphologies of open channels [*Kuiper et al.*, 1966; *Schubert et al.*, 1970] that perhaps formed similar to lava channels in Hawaii and elsewhere on Earth [*Kuiper et al.*, 1966; *Oberbeck et al.*, 1969; *Greeley*, 1971a, 1971b; *Murray*, 1971; *Cruikshank and Wood*, 1972; *Howard et al.*, 1972; *Gornitz*, 1973]. *Hulme* [1973] and *Carr* [1974] first suggested that hot, low-viscosity, perhaps turbulently flowing lavas could incise channels into various substrates on the Moon and Mars by thermal erosion. Since then, many studies have been conducted on the processes of erosion by flowing lava, which includes thermal erosion (melting of country rocks and partial or complete assimilation of the xenomelt into the lava), mechanical erosion (plucking and entrainment of loosely consolidated country materials by the flow), and/or thermomechanical erosion (a combination of these processes). Approaches to study these processes include field studies [*Greeley and Hyde*, 1972; *Lesher*, 1989; *Groves et al.*, 1986; *Greeley et al.*, 1998; *Kauahikaua et al.*, 1998], geochemical analyses of field samples [*Williams et al.*, 2004], petrologic modeling [*Barnes et al.*, 1988; *Lesher and Arndt*, 1995], analog experiments using waxes and slurries [*Huppert and Sparks*, 1985], and computer modeling using fluid dynamic and numerical algorithms [*Huppert and Sparks*, 1985; *Bussey et al.*, 1995, 1997; *Jarvis*, 1995; *Williams et al.*, 1998, 2000a, 2000b, 2001a, 2001b, 2002; *Kerr*, 2001; *Fagents and Greeley*, 2001; *Wilson and Mouginis-Mark*, 2001].

[3] In the case of erosion by lava on Mars, relatively little work has been done due to the lack of knowledge about the

0148-0227/05/2004JE002377$09.00

compositions and rheologies of Martian lavas and the depths and slopes of specific Martian lava channels, as well as the lack of high-resolution coverage of the surface to identify candidate lava erosional channels. Early work focused on numerical modeling based on lunar analogs [*Carr*, 1974] or inferences from terrestrial studies based on limited Viking data [*Cutts et al.*, 1978; *Baird and Clark*, 1984]. *Aguirre-Puente et al.* [1994] modeled thermal erosion of Martian permafrost by water, with a focus on investigating the role of water-induced thermal erosion on the formation of Martian outflow channels. Although the erosional fluid is different, the underlying physics and approach used by *Aguirre-Puente et al.* [1994] has similarities to that of modeling studies of erosion by lava. The most recent investigation of Martian channel formation by lava erosion [*Wilson and Mouginis-Mark*, 2001] took advantage of a numerical model constrained by a high-resolution (~5 m/pixel) Mars Orbiter Camera (MOC) image of a specific channel on the north flank of Elysium Mons, and corresponding Mars Orbiter Laser Altimeter (MOLA) data. The MOC image was used to constrain channel widths and (by shadow measurements) depths, whereas the MOLA data was used to constrain channel elevations and slopes for the numerical modeling.

[4] NASA's Mars Exploration Rovers (MER) and the ESA Mars Express (MEx) orbiter have provided new data to assess erosion by lava. The Spirit and Opportunity rovers have obtained in situ compositional measurements of rocks and soils at two locations on Mars, while the MEx High Resolution Stereo Camera (HRSC) is providing imaging data in color and in stereo, with stereo resolutions better than those of previous missions. Here we report results from the application of an existing model [*Williams et al.*, 1998] to investigate the role of erosion by lava in the formation of Martian channels, using new constraints provided by MER and MEx.

2. Background and Objectives

[5] During the first weeks of operations by the HRSC [*Neukum et al.*, 2004a], a high-resolution (25 m/pixel nadir, 50 m/pixel stereo, 100 m/pixel color) image was obtained over the Elysium volcano Hecates Tholus (Figure 1). Hecates Tholus is a large shield volcano [*Greeley and Spudis*, 1981], ~160 × 175 km in size, whose summit caldera is centered at 32°N, 150°E [*Mouginis-Mark et al.*, 1982]. The caldera appears slightly offset on the volcano, due to flooding by Elysium plains lavas that cover the southwestern part of the shield [*Malin*, 1977; *Mouginis-Mark et al.*, 1982]. Four episodes of caldera collapse are evident [*Mouginis-Mark et al.*, 1982]; crater counts on the new HRSC images suggest that volcanic activity in the caldera occurred as recently as ~100–300 Ma [*Neukum et al.*, 2004b]. Lobate flows were not observed on Hecates in 40 m/pixel Viking images [*Mouginis-Mark et al.*, 1982], but a few flows are visible in the 25 m/pixel HRSC nadir image. A region of reduced crater population (crater sizes <2 km diameter) occurs west of the caldera, which was interpreted as due the presence of a pyroclastic deposit and evidence of explosive volcanism [*Mouginis-Mark et al.*, 1982]. A darker albedo feature in the HRSC color image is also present in this region [*Hauber et al.*, 2005], and in the Mars Odyssey Thermal Emission Imaging System (THEMIS) nighttime infrared mosaic (Figure 2) this region is dark, possibly indicating low thermal inertia materials. It is also at the center of a radial pattern of bright wind streaks visible in the THEMIS nighttime IR data, which has implications for atmospheric behavior around and over Hecates [*Neakrase et al.*, 2005].

[6] Analysis of the HRSC stereo anaglyph of Hecates shows a single, narrow channel emanating from the central caldera that can be traced to the base of the shield, a distance of >66 km. (This channel was recognized in Viking images by *Mouginis-Mark et al.* [1982] and *Gulick and Baker* [1990], although they did not describe it as extending from caldera to base of the shield. In lower-resolution Viking images a central part of the channel appears to be buried by a secondary crater field. In a large photograph of the HRSC stereo anaglyph, the channel can clearly be seen to be continuous underneath the secondary crater ejecta.) The lower reaches of this channel are linear, like most of the other radial channels that cover the lower flanks of the volcano. However, the upper reaches of this channel are quite sinuous and distinct from other channels and depressions on the upper flanks of Hecates. *Fassett and Head* [2004] and C. I. Fassett and J. W. Head III (Valleys on Hecates Tholus, Mars: Origin by basal melting of summit snowpack, submitted to *Planetary and Space Science*, 2005; hereinafter referred to as Fassett and Head, submitted manuscript, 2005) have demonstrated recently that these channels were likely produced by basal melting of a summit snowpack, in which magmatic intrusions within the shield provided heat to melt the overlying snow, producing water that incised the channels on the relatively steeper slopes (5–8°) of the lower shield. This work is consistent with previous studies [e.g., *Mouginis-Mark et al.*, 1982; *Gulick and Baker*, 1990], which concluded that fluvial activity was the most likely explanation for the genesis of the radial Hecates channels. While we do not dispute these findings, the presence of the single, slightly more sinuous channel emanating from the Hecates caldera, and the presence of other collapse features on the upper slopes of the Hecates shield (Figure 1) made us question if lava channels or tubes might have been present on the shield. Such conduits would likely have been exploited by the meltwater of the Fassett and Head model to produce larger, deeper channels on the flanks of the shield. Our experience with the Cave Basalt lava tubes on Mount St. Helens clearly shows that erosion by lava had a role in their formation, and that later surface runoff exploited these tubes [*Greeley and Hyde*, 1972; *Greeley et al.*, 1998; *Williams et al.*, 2004]. Thus this discussion led us to test an alternate hypothesis, that is, whether erosion by lava could have formed (at least in part) the upper reaches of the Hecates channel.

[7] Using numerical modeling constrained by new information on Martian lavas and substrates from current missions, our objectives are to (1) determine the potential for erosion by Martian lavas relative to those on other planets and (2) determine the possibility for lava erosion to produce the Hecates channel and if so, assess the eruption conditions.

3. Methodology

[8] The *Williams et al.* [1998] model of lava emplacement and erosion was developed to assess the potential of

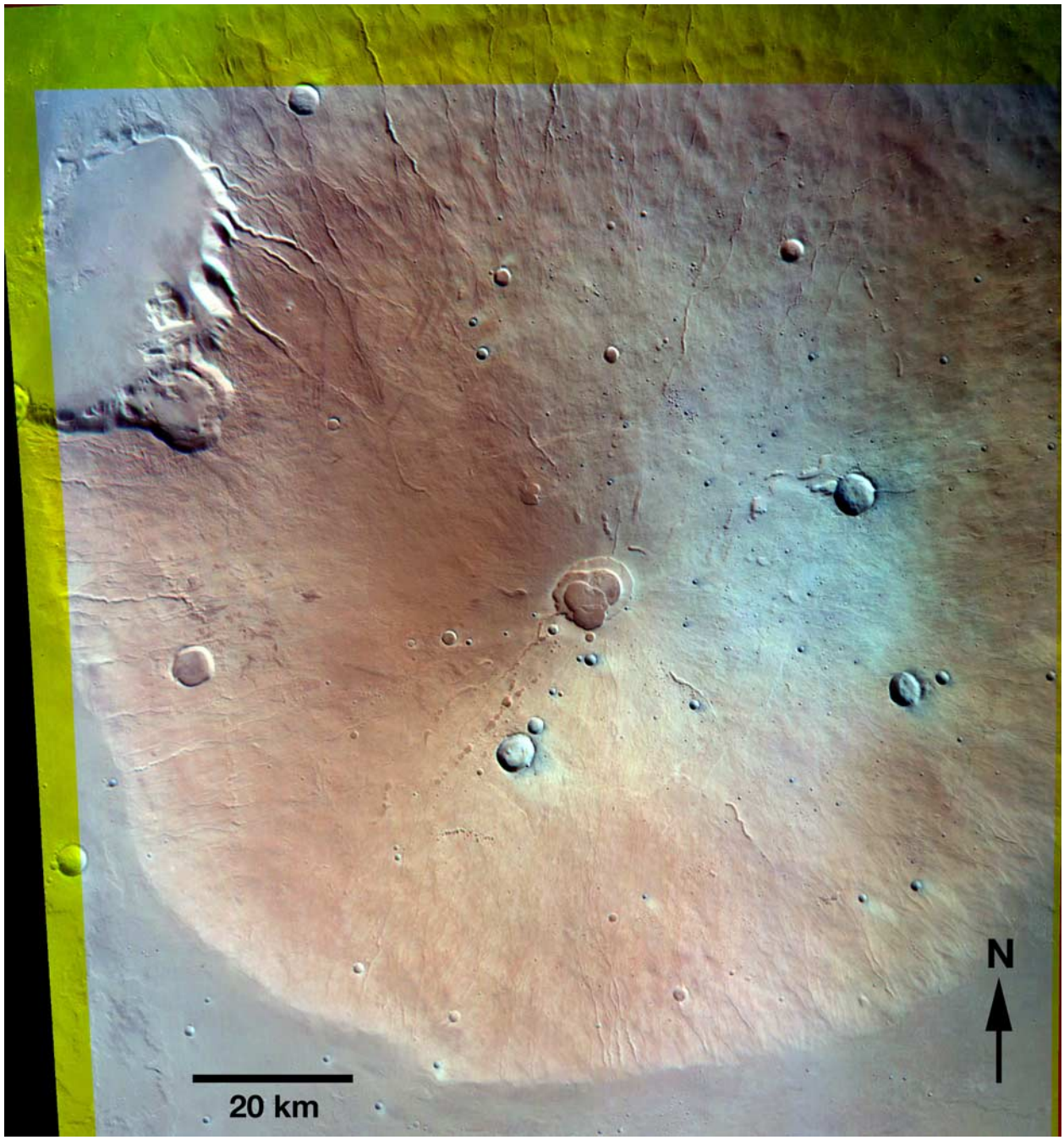

Figure 1. Stretched RGB color image of Hecates Tholus obtained by the High Resolution Stereo Camera (HRSC) on the ESA Mars Express orbiter. The Hecates HRSC images were obtained on orbit 32 on 19 January 2004, with the color channels imaging at 100 m/pixel. This color composite was made using the infrared, green, and blue channels. Note the darker region north and west of the caldera, possibly indicative of the pyroclastic deposits identified by *Mouginis-Mark et al.* [1982]. The white region east of the caldera is thought to consist of clouds, which is consistent with corresponding OMEGA data (F. Poulet, personal communication, 2004). Data from the OMEGA spectrometer on Mars Express also suggest that the darker region of possible pyroclastic material has a different grain size or surface texture than the rest of the shield (F. Poulet, personal communication, 2004).

subaqueously emplaced Precambrian komatiitic lavas to erode channels into substrates of various composition, degrees of consolidation and water content, and adapted to the Moon and Jupiter's moon Io to investigate channel formation on these bodies [*Williams et al.*, 2000a, 2000b, 2001a, 2001b]. However, this model requires as input parameters the major oxide composition of the initial erupted lava and the underlying substrate, as well as an initial flow thickness (proxy for flow rate) and the slope of the underlying substrate. Modeled erosional channel depths

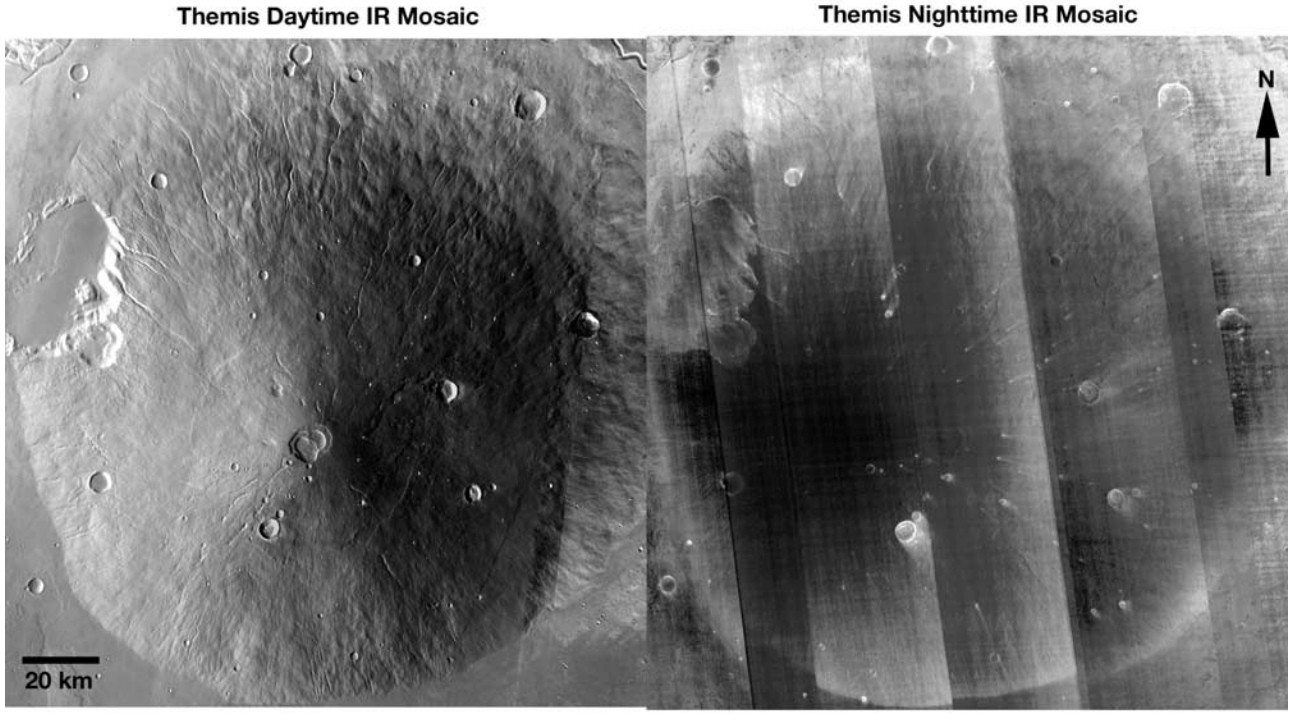

Figure 2. Mars Odyssey THEMIS Infrared (IR) mosaics of Hecates Tholus. (left) Daytime mosaic, processed by the THEMIS Team at Arizona State University. (right) Nighttime mosaic, processed by Dennis Reiss (DLR). A dark region of low thermal inertia materials corresponds roughly with the region containing the pyroclastic deposit of *Mouginis-Mark et al.* [1982]. Interestingly, bright wind streaks emanating from craters are arrayed in a radial pattern centered on this dark region.

as a function of distance from the lava source can be compared with measured depths in the field or image data. This model was applied to the Moon using the compositions of lunar mare basalts [*Williams et al.*, 2000a], and applied to Io using a terrestrial komatiite analog consistent with the Galileo spectral composition and eruption temperature estimates of inferred Ionian ultramafic lavas [*Williams et al.*, 2000b, 2001a]. Until now, there was a lack of good compositional data on Martian basaltic rocks and high-resolution stereo data to determine slopes, flow thicknesses, and channel depths of specific lava channels, data that are now available from MER and MEx.

3.1. Constraints From MER Spirit: Composition of Basaltic Rocks

[9] Spirit landed in Gusev Crater (14°N, 176°E) on Mars on 3 January 2004 [*Squyres et al.*, 2004]. Spirit's early in situ studies focused primarily on the rocks and soils near the landing site using the Microscopic Imager (MI) [*Herkenhoff et al.*, 2004], Alpha-Particle X-ray Spectrometer (APXS) [*Gellert et al.*, 2004; *McSween et al.*, 2004], Mossbauer spectrometer [*Morris et al.*, 2004], and Rock Abrasion Tool (RAT). Although many workers expected Gusev rocks to be sedimentary (from the purported lake sediments that are thought to have flooded the crater [see, e.g., *Kuzmin et al.*, 2000]), the analyzed Gusev rocks show major oxide compositions consistent with primitive basalts, comparable "with terrestrial basaltic komatiites" [*Gellert et al.*, 2004]. Such compositions are ideal proxies for mafic lava compositions in our modeling. Furthermore, *McSween et al.* [2004] reported extrapolated compositions for these rocks that were brushed to remove dust coatings, that were ground to remove thin silica coatings (providing unaltered surfaces for study), and that were adjusted for soil sulfur content. For our modeling, we chose the Adirondack end-member [see *McSween et al.*, 2004, Table 1], which was the most mafic composition reported. Compared to terrestrial basalts (Table 1), the Gusev basalts are lower in silica and alumina, higher in magnesia, and much higher in iron. In fact, if the Gusev rocks occurred on Earth, then they would be classified as high-Mg basalts (i.e., 9–12 wt% MgO). These results are consistent with earlier work by *Baird and Clark* [1981], who suggested that the "silicate fraction" of Martian fines analyzed by the Viking landers had a composition likely derived from "Fe-rich komatiite-like basalts."

[10] If we assume (for modeling purposes) that a Martian liquid lava had the composition of the Gusev basalts, then it would have had a 1-bar liquidus temperature ~1270°C (based on calculations using MELTS [*Ghiorso and Sack*, 1995] on this composition, assuming fO_2 constrained by the QFM buffer), a density of ~2820 kg/m^3, and a dynamic viscosity (at liquidus) of ~2 Pa·s (similar to glycerin). For lavas with such a low-viscosity, it is likely that they could have been emplaced as turbulent flows (Reynolds number >2000 for confined flow), even at relatively low flow rates [*Williams et al.*, 1998, 1999].

3.2. Constraints From MEx: Slopes, Flow Thicknesses, and Channel Depths

[11] HRSC imaging data obtained for Hecates Tholus include nearly complete nadir coverage at 25 m/pixel, stereo coverage at 50 m/pixel, and 4-color coverage at 100 m/pixel

Table 1. Compositions of Several Planetary Lava Analogs With Corresponding Thermal-Rheological Properties for Liquids Based on These Compositions[a]

Component/Parameter	Mars: Gusev Crater Basalt	Earth: Cave Basalt	Earth: Katinniq Komatiitic Basalt	Earth: Kambalda Komatiite	Moon: Low-TiO_2 Mare Basalt	Io: Ultramafic Lava Analog
SiO_2	45.4	49.5	46.9	45.0	43.6	49.8
TiO_2	0.46	1.50	0.6	0.3	2.6	0.1
Al_2O_3	10.9	17.4	9.8	5.6	7.9	7.9
Fe_2O_3	3.02	11.5	-	1.4	-	0.5
FeO	15.2	0.0	14.4	9.2	21.7	4.8
MnO	0.41	0.16	0.3	0.2	0.3	0.1
MgO	12.8	6.85	18.9	32.0	14.9	30.9
CaO	7.49	9.64	8.6	5.3	8.3	5.2
Na_2O	2.79	3.44	0.3	0.6	0.2	0.4
K_2O	0.06	0.50	0.05	0.03	0.05	0.1
T_{liq}, °C	1270	1205	1419	1638	1440	1611
T_{sol}, °C	1150	1050	1150	1170	1150	1170
ρ at T_{liq}, kg/m^3	2820	2510	2800	2770	2900	2680
c, J/kg.°C	1560	1560	1640	1790	1570	1780
μ at T_{liq}, Pa·s	2.3	63–68	0.74	0.08	0.40	0.22
L at T_{liq}, J/kg	7.05E + 05	5.01E + 05	5.96E + 05	6.97E + 05	6.06E + 05	6.84E + 05
Composition location	Adirondack composite[b]	Mount St. Helens, Wash.	Cape Smith Belt, Canada	Western Australia	Ap.12 Sample 12002	South Africa
Reference	*McSween et al.* [2004]	*Williams et al.* [2004]	*Barnes et al.* [1982]	adapted from *Lesher and Arndt* [1995]	*Walker et al.* [1976]	*Wilson and Carlson* [1989]

[a]Liquidus temperatures (T_{liq}) were calculated using MELTS [*Ghiorso and Sack*, 1995]; the solidus temperatures (T_{sol}) are taken from the experimental data of *Arndt* [1976]. Density (ρ) was calculated using the method of *Bottinga and Weill* [1970] with the coefficients of *Mo et al.* [1982]; liquid viscosity (μ) was calculated using the method of *Shaw* [1972]; specific heat (c) was calculated from the heat capacity data of *Lange and Navrotsky* [1992]; and heat of fusion (L) is approximated using data from *Navrotsky* [1995].

[b]A subsequent recalibration of the Spirit APXS data suggests slight changes in some major oxides, but the values would not have a significant impact on the modeled rheological properties.

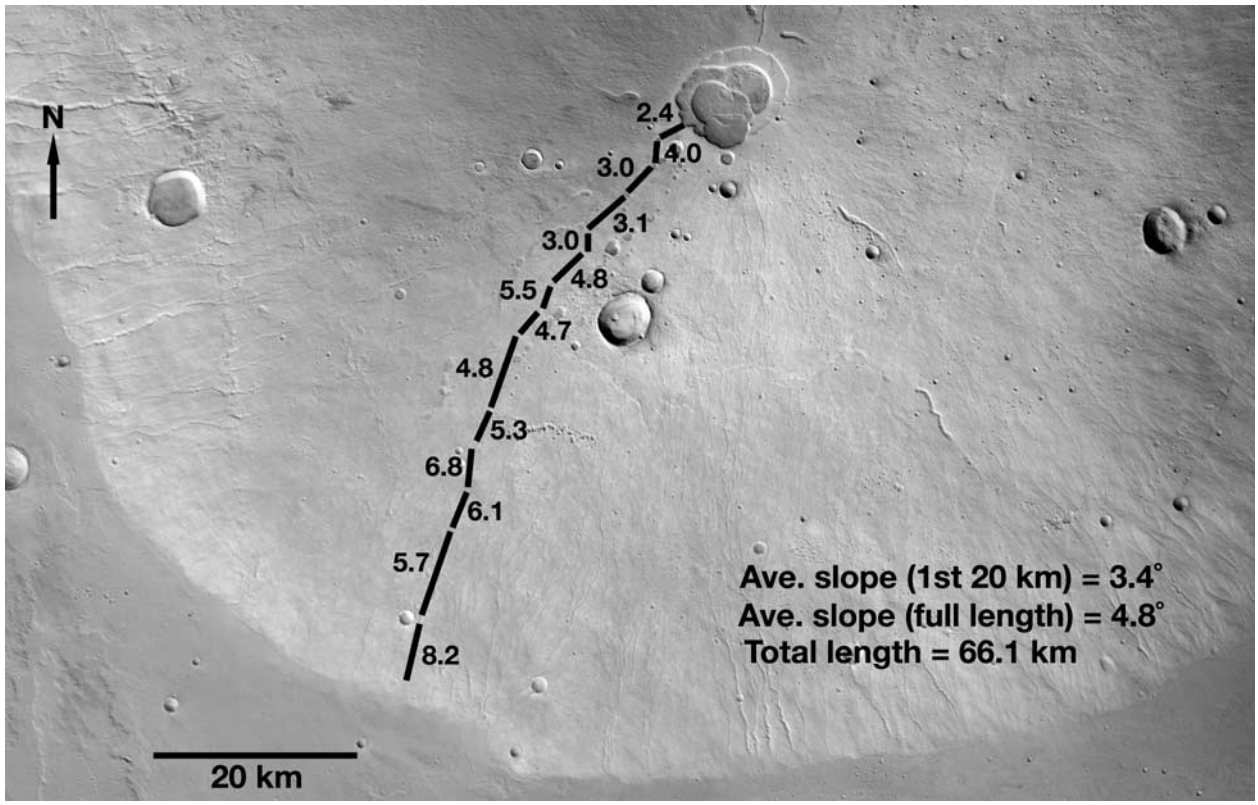

Figure 3. A portion of the HRSC nadir image of Hecates Tholus, showing where slope measurements were made within the channel using the 100 m DTM. Slope measurements in degrees. The slopes are shallow close to the caldera but steepen considerably on the flanks of the shield.

(Figure 1). (The HRSC is a push-broom imaging camera that obtains long image strips under its orbit track near periapsis, with best resolutions of typically 15-18 m per pixel. The HRSC provides near-simultaneous imaging using 9 channels, including nadir, forward-looking, and backward-looking stereo, four color channels (red, green, blue, infrared), and two photometry channels. In addition, a separate Super-Resolution Channel (SRC) obtains monochrome image frames embedded in the HRSC image strips at resolutions of 2–5 m per pixel. For more information on the HRSC experiment, see *Neukum et al.* [2004a].) These images were processed to produce a red-green stereo anaglyph, and a Digital Terrain Model (DTM) with a spatial resolution of 100 m/px. We used the HRSC DTM to determine the slope of the Hecates channel in segments along its length (Figure 3). Nearest the caldera the slope in the channel is ~2.4°, but quickly increases to 3–5° on the upper flanks of the volcano. The slope generally increases on the lower flanks, from 5–6° to more than 8° at the base of the shield. The average slope along the channel (summing the segments given in Figure 3) is 4.8°, and is 3.4° over the first ~20 km of the channel. On the basis of error propagation calculations which take into account the mean 3D point accuracy and the horizontal separations involved, we can estimate a mean angular accuracy of about one fourth of a degree for the slope values. The expected error is smaller than 0.5° for all derived slopes. These slope values serve as an input parameters for our model.

[12] The channel ranges in width from ~520 m at the channel head in the caldera wall to ~180 m near the point where it starts to disappear in the secondary crater field (Figures 4–6). Shadow measurement of channel depth from the HRSC resampled nadir image at 12.5 m/pixel (Figure 4 and Table 2) show that the channel is as deep as ~105 m near the channel head gradually decreasing to a few tens of meters deep about 20 km from the head. As a check on the shadow measurements, we also attempted to measure channel depths on the stereo comparator. This device allows precise determination (few microns) of the parallax differences between the heights of surface features, if performed by an experienced user. One of us (G.N.) made several depth measurements in the channel (Table 2 and Figure 4), which were calibrated to points in the Hecates caldera along a MOLA track. These results are consistent with our shadow measurements, in that the widest parts of the channel in the first 20 km downstream are ~40–60 m deep.

[13] We also determined flow thickness from shadow measurements of a few visible flow fronts (Table 2: ~20–60 m thick). Because lava flows generally increase in thickness as they flow downstream (i.e., eroding flows assimilate substrate and grow crusts on their upper surfaces, and tube-fed flows grow by inflation [*Hon et al.*, 1994]), these thicknesses place upper bounds on the initial flow thicknesses in our model. Flow thickness is used as a proxy for flow rate, assuming constant flow rate downstream [*Williams et al.*, 1998].

3.3. Model Description

[14] The *Williams et al.* [1998] lava emplacement and erosion model has been adapted for Martian gravity and

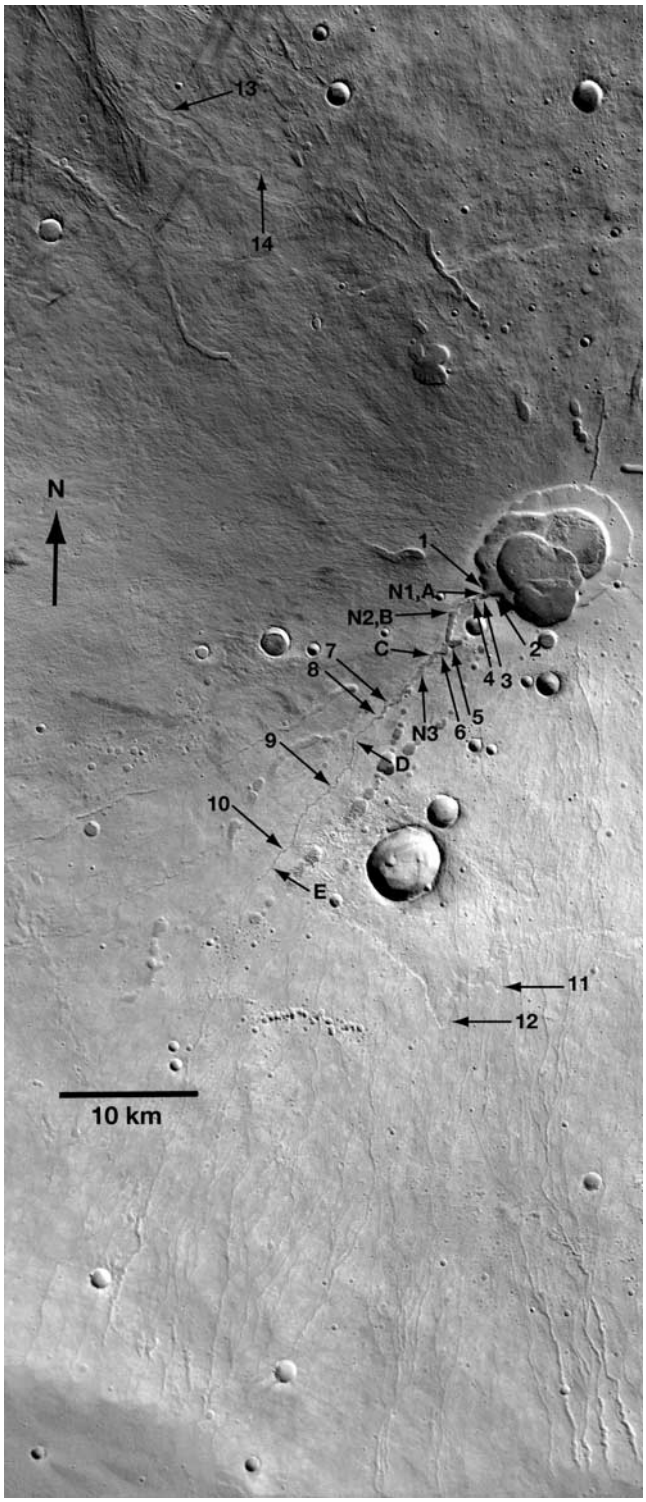

Figure 4. Locations of shadow measurements made on the HRSC nadir (12.5 m/pixel) image of the main Hecates channel. Numbers refer to the measurements in Table 2. Numbers 1–10 and N1-N3 are channel depth measurements, numbers 11–14 are flow lobe thicknesses, and letters A–E are channel width measurements.

environment. Because a detailed description of this model has been previously published [*Williams et al.*, 1998, 1999, 2000a, 2000b], only a brief description is given here. The model begins at the vent with the input of an initial lava composition, substrate composition (here assumed to be the same as the lava), liquidus, solidus, and eruption temperatures (Table 1), surface pressure, flow thickness, ground slope, and fraction of water ice in the substrate. A series of algorithms is used to calculate the initial thermal-physical properties of the lava (dynamic viscosity, density, specific heat, heat of fusion, etc.; see Table 1). From the initial values of the lava thermal-physical properties, a series of auxiliary equations is used to calculate additional lava properties at the vent including crystallinity, bulk viscosity, flow velocity, friction coefficient, Reynolds number, Prandtl number, convective heat transfer coefficient, erosion rate, and the degree of contamination of the lava by assimilated substrate. The compositional change in the liquid lava due to the assimilation of thermally eroded substrate is calculated using mass balance expressions, as is the compositional change in the liquid lava due to the crystallization of olivine. These mass balance expressions are used to calculate a new liquid lava composition that is used to recalculate the temperature- and composition-dependent thermal, rheological, and fluid dynamic properties of the lava at each model increment. The decrease in lava temperature due to convective heat transfer, formation of a coherent crust, and thermal erosion at the base of the flow (including release of latent heat) is calculated using a first-order ordinary differential equation modified from *Huppert and Sparks* [1985]. Because the physical properties of the lava are changing with downstream flow, this equation must be solved at each increment of distance from the eruption source using a fourth-order Runge-Kutta numerical method. Once a new temperature and a new lava composition are calculated, all of the important thermal, rheological, and fluid dynamic parameters are recalculated at the next increment of distance downstream. Thus the thermal, fluid dynamic, and geochemical evolution of the lava flow with distance is simulated [*Williams et al.*, 1998, 1999, 2000a, 2000b].

3.4. Modeling Assumptions

[15] We make several additional assumptions about other relevant parameters. For this work, we are interested in determining erosion in the first 30 km or so from the vent. Other model output for which there are no field data for comparison in the Martian case (e.g., lava crustal thicknesses in the channel, degree of contamination in sampled flows, etc.) are not reported or discussed. Furthermore, the substrate composition is assumed to be similar to the overlying lava, which is not unreasonable for flows on the top of a volcanic edifice. We assume that no inflation occurs in the channel during lava emplacement. The lavas are assumed to erupt and flow over an unobstructed homogeneous substrate, but with a slope determined from the HRSC DTM. Because results from the Gamma Ray Spectrometer on the Mars Odyssey orbiter suggest the widespread presence of water ice in the Martian regolith [*Boynton and the GRS Team*, 2002; *Feldman et al.*, 2002], because recent models suggest cyclical variations in Martian climate enabling the accumulation of snowpacks on some parts of the surface [*Mischna et al.*, 2003], and because

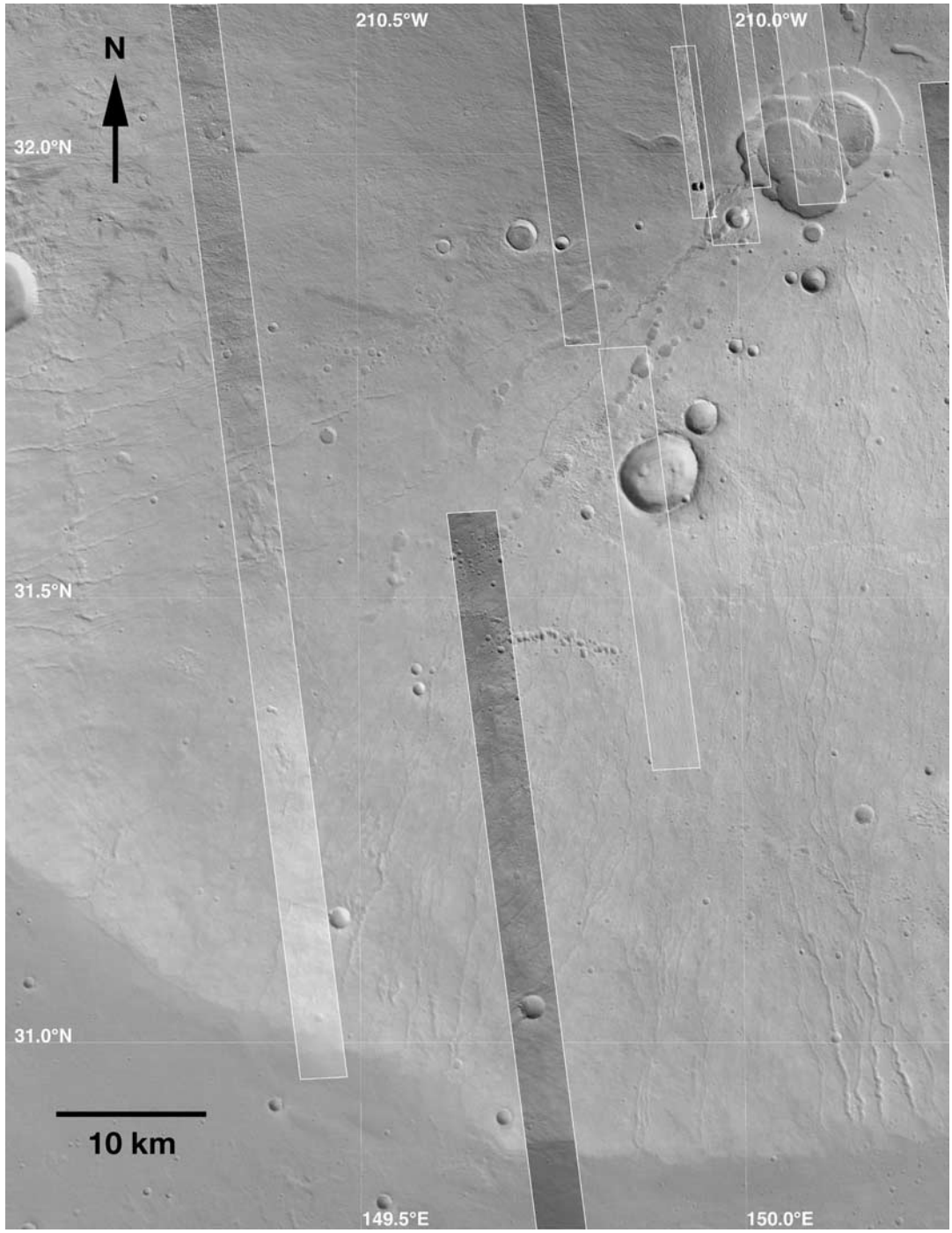

Figure 5. Mars Global Surveyor MOC-NA imaging (2–6 m/pixel) coverage of the Hecates caldera and main channel, superposed on HRSC nadir image (12.5 m/pixel). Coverage is quite irregular over the channel, and there were no useful shadows to obtain depth measurements, necessitating the use of the HRSC nadir image.

there is compelling evidence for basaltic pyroclastic material on Hecates Tholus [*Mouginis-Mark et al.*, 1982], it seems reasonable to test erosional models for both erosion of a pure basaltic substrate, and for a substrate consisting of both basalt and ice (perhaps analogous to a pyroclastic deposit with ice filling the voids between rock fragments). For simplicity, we assume that the pure lava substrate begins to melt at a single temperature (1080°C), which for this composition has a corresponding liquid viscosity of 17 Pa·s. In reality, as the substrate is heated the lower melting temperature glasses and mineral components (e.g., feldspar) are the first to melt, which probably reduce the strength of the ground such that the remaining material can be removed by mechanical erosion. For the 50% ice-50% rock substrate, we assume it is consolidated, and that the ice is melted first followed by the rock. When more

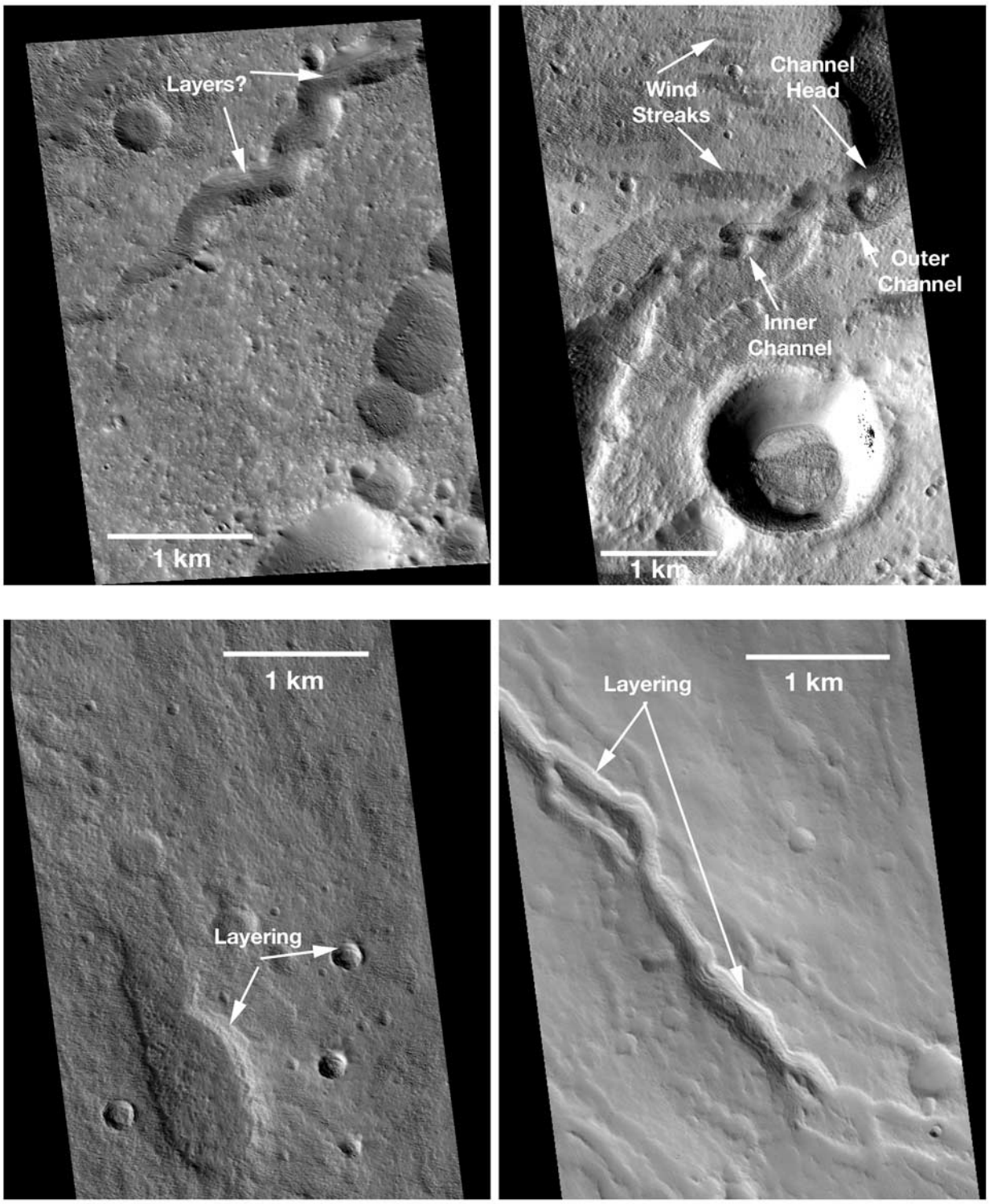

Figure 6. Mars Global Surveyor MOC-NA images showing surface textures and layering on Hecates Tholus. All images are 3.13 km wide. (top left) Part of the main channel, with potential layering of volcanic materials exposed in the channel's walls (from image M0802738, 6.1 m/px). (top right) The channel head is a breach in the caldera wall, and distinct outer and sinuous inner channels can be seen (from image M1801860, 3.1 m/px). (bottom left) A collapse pit and impact craters show layering in their walls (from image M0303180, 3.1 m/px). (bottom right) One of the likely fluvial channels on the northern flank, showing layering in the channel walls (from image M0802738, 6.1 m/px). North is up in all images.

Table 2. Measurements of Channel Depths and Widths and Nearby Flow Lobe Thicknesses for the Hecates Channel[a]

Measurement	Type of Feature	Type of Measurement	Value, m
1	channel depth	shadow	170
2	"	"	105
3	"	"	84
4	"	"	74
5	"	"	105
6	"	"	95
7	"	"	63
8	"	"	63
9	"	"	42
10	"	"	32
11	flow thickness	"	32
12	"	"	21–32
13	"	"	32–63
14	"	"	32–53
A	channel width	"	520
B	"	"	760
C	"	"	400
D	"	"	175
E	"	"	185
N1	channel depth	parallax	40–60
N2	"	"	60
N3	"	"	20–40

[a]For locations, refer to Figure 4.

information about the mineralogy of Martian basalts becomes available, more sophisticated algorithms to simulate substrate melting can be employed.

4. Results and Discussion

[16] We report model results in the form of graphs showing erosion rate and erosion depth after one month of flow versus distance from source. To investigate our first question, "What was the potential for erosion by Martian lavas relative to those on other planets?", we ran our model using the Gusev composition in Table 1 for both lava and substrate, erupting the lava at its liquidus for a 10 m thick flow over a substrate slope of 0.1° at ambient temperature (for Mars, −59°C [*Lodders and Fegley*, 1998]) and assuming no water or ice in the substrate. These "baseline parameters" facilitate comparison between different lava compositions on different planets [e.g., *Williams et al.*, 1998, 2000a, 2000b]. These results are given in Figure 7. Compared to highly ultramafic lavas, such as terrestrial high-MgO komatiites, Martian lavas (based on the MER Spirit compositions from Gusev) are much less mafic, and thus have higher viscosities, lower potentials for turbulence, and thus lower erosion rates. These results are consistent with previous findings of sensitivity analyses of this model [*Williams et al.*, 1999]. In general, erosional potential of low-viscosity lavas increases with MgO and FeO content, flow rate, slope, and degree of unconsolidation and the presence of low melting temperature volatiles (i.e., water) in the underlying substrate. Interestingly, these results indicate that Martian basalts are slightly more erosive than lunar mare basalts (initial rates of 17 versus 13 cm/d), even though the lunar mare basalts have higher combined MgO and FeO contents, higher liquidus temperature, and lower dynamic viscosity (Table 1). The reason for this is that at this flow rate and slope, the convective heat transfer rate to the substrate is higher in the Martian case because of the higher Prandtl number. For other initial conditions (higher flow rate or steeper slope), the higher temperature, lower viscosity of lunar lavas would dominate and result in higher heat transfer rates and erosion rates than the Martian lavas.

[17] To investigate our second question, "Was it possible for erosion by lava to produce (at least the upper reaches of) the Hecates channel?", we ran our model using the Gusev composition in Table 1 for both lava and substrate, erupting the lava at its liquidus for three different initial flow thicknesses ("thin": 3 m, "intermediate": 7.5 m, and "thick": 15 m thick flows) over a slope of 3.4° (consistent with the steeper slope as determined from the HRSC DTM), at an ambient temperature of −59°C. We performed model runs assuming no ice in the substrate, and 50% ice in the substrate (Table 3, Figure 8). Our results show, as expected, higher erosion rates at higher flow rates, and higher erosion rates of substrate made up of ice and rock than just rock alone. Over a substrate of rock alone, thin, intermediate, and thick Martian lava flows (as defined above) produce initial erosion rates of roughly 50, 75, and 90 cm/d, respectively. To erode a 100 m deep channel (depth near the channel head) at these rates would require ~200, 130, and 110 days (~4–7 months), respectively. If the substrate contained a significant fraction of water ice (50%), thin, intermediate, and thick Martian lava flows (as defined above) produce initial erosion rates of 102, 150, and 190 cm/d, respectively. To erode a 100 m deep channel would require ~98, 67, and 53 days, respectively. To erode a 40 m deep channel at these erosion rates would have required eruption durations of

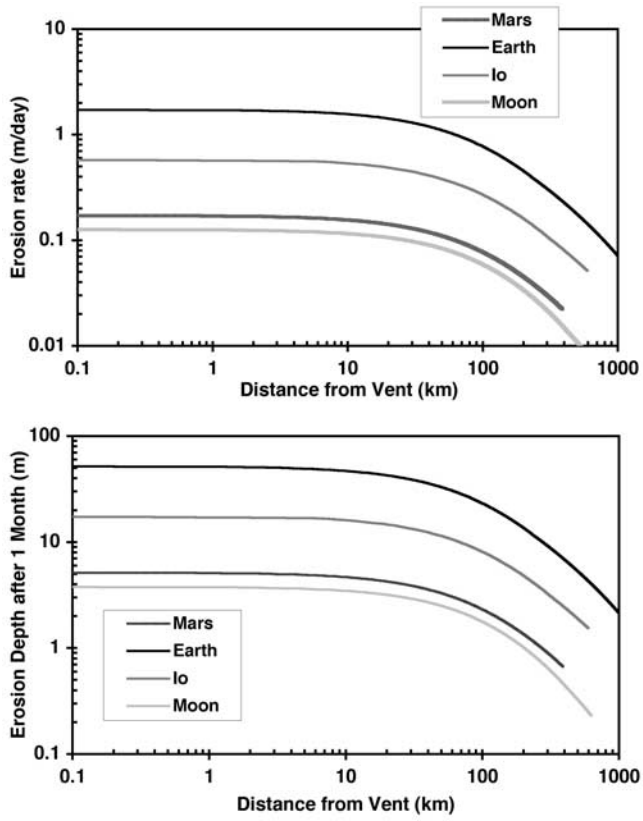

Figure 7. Graph of model results comparing the erosional potential of lavas based on the Gusev compositions to lunar mare basalts, terrestrial komatiites, and hypothesized Ionian ultramafic lavas.

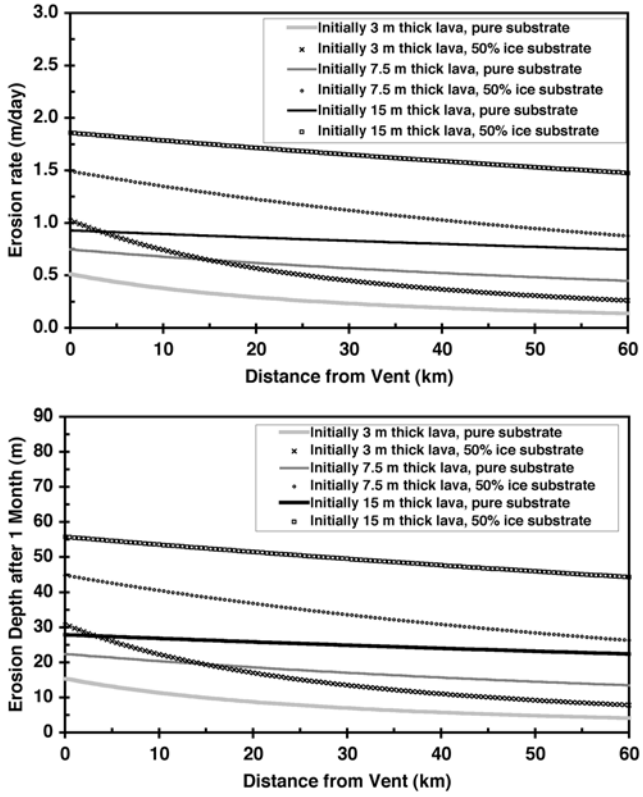

Figure 8. Graph of model results comparing the erosional potential of Martian lavas for three different flow thicknesses (flow rates) and rock-ice substrate mixtures.

~80, 53, and 44 days (for thin, intermediate, and thick flows over rock substrate, respectively), and ~39, 27, and 21 days (for thin, intermediate, and thick flows over rock and ice substrate, respectively). Although no active Martian basaltic volcanism has ever been detected, if we assume similar eruption durations occurred on Mars as on Earth, then these eruption durations are not unreasonable. *Kauahikaua et al.* [1998] has documented continuous or nearly continuous laminar flow of lava in Hawaiian lava tubes, including downcutting by thermal erosion at a rate of ~10 cm/d lasting for weeks to months. Tube- and channel-fed eruptions from other terrestrial basaltic volcanoes (Etna) are known to have had durations of days to weeks. Furthermore, our model results for "thin" and "intermediate" flows are consistent with the results of *Wilson and Mouginis-Mark* [2001] for the formation of a lava channel by thermal erosion on Elysium Mons; their flow rates (~3,400–13,000 m^3/s), erupted volumes (~29–39 km^3), and eruption durations (~40–130 days) are similar to our values (flow rates: ~5300–25,000 m^3/s, erupted volumes: ~14–64 km^3, eruption durations: ~30–200 days, depending on depth of erosion).

[18] It seems likely that Martian lavas were capable of producing erosional channels if erupted lavas were above or near their liquidi, if they contained few entrained crystals and/or a low abundance of vesicles, if they flowed over relatively steep slopes (>1°), if the substrates were loosely or unconsolidated (and mixed with ice), and if eruption durations were weeks to months in length. In the case of the large channels on Hecates Tholus, if

Table 3. Model Results for Simulations of Erosion by Lava on Hecates Tholus[a]

Parameter	3 m Thick Flow, Pure Substrate	3 m Thick Flow, 50% Ice Substrate	7.5 m Thick Flow, Pure Substrate	7.5 m Thick Flow, 50% Ice Substrate	15 m Thick Flow, Pure Substrate	15 m Thick Flow, 50% Ice Substrate
Flow rate,[b] m^3/s	5.3E + 03	5.3E + 03	2.5E + 04	2.5E + 04	7.7E + 04	7.7E + 04
Initial Reynolds number	7.2E + 04	7.2E + 04	4.0E + 05	4.0E + 05	1.3E + 06	1.3E + 06
Initial erosion rate, cm/d	51	102	75	150	93	190
Initial Erosion Depth (after 1 month, m)	15	31	22	45	28	56
Erosion rate @20 km downstream, cm/d	29	57	62	120	86	170
Erosion depth @20 km downstream (after 1 month), m	8.7	17	19	37	26	52
Erupted volume (after 1 month),[c] km^3	14	14	64	64	201	201

[a]Refer to Figure 8.
[b]Flow Rate = Flow Velocity × Flow Thickness × 150 m (average channel width).
[c]Erupted Volume = Flow Rate × 2.592E + 06 seconds s (1 month).

conduit-fed flow occurred, the production of channels and tubes at least partially formed by erosion by lava would have served as conduits for later meltwaters, resulting in larger fluvial channels on the lower flanks of the shield as described by *Fassett and Head* [2004, submitted manuscript, 2005]. To better understand the potential role of erosion by lava and other volcanic processes on Mars will require more study using the new data sets now being returned by MER and Mars Express, as well as more in situ compositional data from additional volcanic sites on Mars, and higher-resolution imaging of volcanic terrains such as that which will be provided by the 2005 Mars Reconnaissance Orbiter.

[19] **Acknowledgments.** The investigation by D.A.W. and R.G. was supported by NASA through the Planetary Geology and Geophysics Program and a contract from the Jet Propulsion Laboratory for participation in the Mars Express project. We are grateful for the excellent work by the Mars Express flight team and the HRSC groups at DLR and FU-Berlin in obtaining the data to enable the study. The authors would like to thank members of the HRSC Co-Investigator Team for their input, Dennis Reiss of DLR for processing the THEMIS night time IR mosaic, and Frank Scholten and Marita Wählisch of DLR for the production of the HRSC stereo anaglyph that motivated this work.

References

Aguirre-Puente, J., F. Costard, and R. Posado-Cano (1994), Contribution to the study of thermal erosion on Mars, *J. Geophys. Res.*, *99*, 5657–5667.

Arndt, N. T. (1976), Melting relations of ultramafic lavas (komatiites) at one atmosphere and high pressure, *Year Book Carnegie Inst. Washington*, *75*, 555–562.

Baird, A. K., and B. C. Clark (1981), On the original igneous source of Martian fines, *Icarus*, *45*, 113–123.

Baird, A. K., and B. C. Clark (1984), Did komatiitic lavas erode channels on Mars?, *Nature*, *311*, 18.

Barnes, S. J., C. J. A. Coats, and A. J. Naldrett (1982), Petrogenesis of a Proterozoic nickel sulfide-komatiite association: The Katiniq Sill, Ungava, Quebec, *Econ. Geol.*, *77*, 413–429.

Barnes, S. J., R. E. T. Hill, and M. J. Gole (1988), The Perseverance Ultramafic Complex, Western Australia: The product of a komatiite lava river, *J. Petrol.*, *29*, 302–331.

Bottinga, Y., and D. F. Weill (1970), Densities of liquid silicate systems calculated from partial molar volumes of oxide components, *Am. J. Sci.*, *269*, 169–182.

Boynton, W. V., and the GRS Team (2002), Distribution of hydrogen in the near-surface of Mars: Evidence for subsurface ice deposits, *Science*, *297*, 71–75.

Bussey, D. B. J., S.-A. Sørensen, and J. E. Guest (1995), Factors influencing the capability of lava to erode its substrate: Application to Venus, *J. Geophys. Res.*, *100*, 16,941–16,948.

Bussey, D. B. J., S.-A. Sørensen, and J. E. Guest (1997), On the role of thermal conductivity on thermal erosion by lava, *J. Geophys. Res.*, *102*, 10,905–10,908.

Carr, M. H. (1974), The role of lava erosion in the formation of lunar rilles and Martian channels, *Icarus*, *22*, 1–23.

Cruikshank, D. P., and C. A. Wood (1972), Lunar rilles and Hawaiian volcanic features: Possible analogs, *Moon*, *3*, 412–447.

Cutts, J. A., W. J. Roberts, and K. R. Blasius (1978), Martian channels formed by lava erosion (abstract), *Lunar Planet. Sci.*, *IX*, 209.

Fagents, S. A., and R. Greeley (2001), Factors influencing lava-substrate heat transfer and implications for thermomechanical erosion, *Bull. Volcanol.*, *62*, 519–532.

Fassett, C. I., and J. W. Head III (2004), Snowmelt and the formation of valley networks on Martian volcanoes, *Lunar Planet. Sci.* [CD-ROM], *XXXV*, abstract 1113.

Feldman, W. C., et al. (2002), Global distribution of neutrons from Mars: Results from Mars Odyssey, *Science*, *297*, 75–78.

Gellert, R., et al. (2004), Chemistry of rocks and soils in Gusev Crater from the Alpha Particle X-ray Spectrometer, *Science*, *305*, 829–832.

Ghiorso, M. S., and R. O. Sack (1995), Chemical mass transfer in magmatic processes IV. A revised and internally consistent thermodynamic model for the interpolation and extrapolation of liquid-solid equilibria in magmatic systems at elevated temperatures and pressures, *Contrib. Mineral. Petrol.*, *119*, 197–212.

Gornitz, V. (1973), The origin of sinuous rilles, *Moon*, *6*, 337–356.

Greeley, R. (1971a), Lunar Hadley Rille: Considerations of its origins, *Science*, *172*, 722–725.

Greeley, R. (1971b), Lava tubes and channels in the lunar Marius Hills, *Moon*, *3*, 289–314.

Greeley, R., and J. H. Hyde (1972), Lava tubes of the Cave Basalt, Mount St. Helens, Washington, *Geol. Soc. Am. Bull.*, *83*, 2397–2418.

Greeley, R., and P. D. Spudis (1981), Volcanism on Mars, *Rev. Geophys.*, *19*, 13–41.

Greeley, R., S. A. Fagents, R. S. Harris, S. D. Kadel, D. A. Williams, and J. E. Guest (1998), Evidence for erosion by flowing lava and planetary implications, *J. Geophys. Res.*, *103*, 27,325–27,346.

Groves, D. I., E. A. Korkiakoski, N. J. McNaughton, C. M. Lesher, and A. Cowden (1986), Thermal erosion by komatiites at Kambalda, Western Australia and the genesis of nickel ores, *Nature*, *319*, 136–139.

Gulick, V. C., and V. R. Baker (1990), Origin and evolution of valleys on Martian volcanoes, *J. Geophys. Res.*, *95*, 14,325–14,344.

Hauber, E., et al. (2005), Discovery of a flank caldera and very young glacial activity at Hecates Tholus, Mars, *Nature*, *434*, 356–361.

Herkenhoff, K. E., et al. (2004), Textures of the soils and rocks at Gusev crater from Spirit's Microscopic Imager, *Science*, *305*, 824–826.

Hon, K., J. Kauahikaua, R. Delinger, and K. Mackay (1994), Emplacement and inflation of pahoehoe sheet flows: Observations and measurements of active lava flows on Kilauea Volcano, Hawaii, *Geol. Soc. Am. Bull.*, *106*, 351–370.

Howard, K. A., J. W. Head, and G. A. Swann (1972), Geology of Hadley Rille, *Proc. Lunar Sci. Conf. 3rd*, 1–14.

Hulme, G. (1973), Turbulent lava flows and the formation of lunar sinuous rilles, *Mod. Geol.*, *4*, 107–117.

Huppert, H. E., and R. S. J. Sparks (1985), Komatiites, I, Eruption and flow, *J. Petrol.*, *26*, 694–725.

Jarvis, R. A. (1995), On the cross-sectional geometry of thermal erosion channels formed by turbulent lava flows, *J. Geophys. Res.*, *100*, 10,127–10,140.

Kauahikaua, J., K. Cashman, K. Hon, T. Mattox, C. Heliker, M. Mangan, and C. Thornber (1998), Observations on basaltic lava streams in tubes from Kilauea volcano, Hawai'i, *J. Geophys. Res.*, *103*, 27,303–27,324.

Kerr, R. C. (2001), Thermal erosion by laminar lava flows, *J Geophys Res.*, *106*, 26,453–26,465.

Kuiper, G. P., R. G. Strom, and R. S. Le Poole (1966), Interpretation of Ranger records, in *Ranger VIII and IX, Part II, Experimenters' Analyses and Interpretations*, *Jet Propul. Lab. Tech. Rep. 32–800*, pp. 35–248, Calif. Inst. of Technol., Pasadena.

Kuzmin, R. O., R. Greeley, R. Landheim, N. A. Cabrol, and J. D. Farmer (2000), Geologic map of the MTM-15182 and MTM-15187 quadrangles, Gusev Crater-Ma'adim Vallis region, Mars, 1:500,000, *U.S. Geol. Surv. Geol. Invest. Ser., Map I-2666*.

Lange, R. A., and A. Navrotsky (1992), Heat capacities of Fe_2O_3-bearing silicate liquids, *Contrib. Mineral. Petrol.*, *110*, 311–320.

Lesher, C. M. (1989), Komatiite-associated nickel sulfide deposits, in *Ore Deposits Associated With Magmas*, edited by J. A. Whitney and A. J. Naldrett, *Rev. Econ. Geol.*, *4*, 45–102.

Lesher, C. M., and N. T. Arndt (1995), REE and Nd geochemistry, petrogenesis, and volcanic evolution of contaminated komatiites at Kambalda, Western Australia, *Lithos*, *34*, 127–158.

Lodders, K., and B. Fegley Jr. (1998), *The Planetary Scientist's Companion*, 371pp., Oxford Univ. Press, New York.

Malin, M. C. (1977), Comparison of volcanic features of Elysium (Mars) and Tibesti (Earth), *Geol. Soc. Am. Bull.*, *88*, 908–919.

McSween, H. Y., et al. (2004), Basaltic rocks analyzed by the Spirit rover in Gusev crater, *Science*, *305*, 842–845.

Mischna, M. A., M. I. Richardson, R. J. Wilson, and D. J. McCleese (2003), On the orbital forcing of Martian water and CO_2 cycles: A general circulation model study with simplified volatile schemes, *J. Geophys. Res.*, *108*(E6), 5062, doi:10.1029/2003JE002051.

Mo, X., I. S. E. Carmichael, M. Rivers, and J. Stebbins (1982), The partial molar volume of Fe_2O_3 in multicomponent silicate liquids and the pressure dependence of oxygen fugacity in magmas, *Mineral. Mag.*, *45*, 237–245.

Morris, R. V., et al. (2004), Mineralogy at Gusev crater from the Mössbauer spectrometer on the Spirit rover, *Science*, *305*, 833–836.

Mouginis-Mark, P. J., L. Wilson, and J. W. Head III (1982), Explosive volcanism on Hecates Tholus, Mars: Investigation of eruption conditions, *J. Geophys. Res.*, *87*, 9890–9904.

Murray, J. B. (1971), Sinuous rilles, in *Geology and Physics of the Moon: A Study of Some Fundamental Problems*, edited by G. Fielder, chap. 3, pp. 27–39, Elsevier, New York.

Navrotsky, A. (1995), Energetics of silicate melts, in *Structure, Dynamics and Properties of Silicate Melts*, edited by J. F. Stebbins, P. F. McMillan, and D. B. Dingwell, *Rev. Mineral.*, *32*, 121–142.

Neakrase, L. D. V., R. Greeley, D. A. Williams, D. Reiss, T. I. Michaels, S. C. R. Rafkin, G. Neukum, and the HRSC Co-Investigator Team (2005), Hecates Tholus, Mars: Nighttime aeolian activity suggested by thermal images and mesoscale atmospheric model simulations, *Lunar Planet. Sci.* [CD-ROM], *XXXV*, abstract 1898.

Neison, E. (1876), *The Moon*, pp. 73 and 275, Pitman, London.

Neukum, G., R. Jaumann, and the HRSC Co-Investigator and Experiment Teams (2004a), HRSC: The High Resolution Stereo Camera on Mars Express, *Eur. Space Agency Spec. Publ., ESA-SP. 1240*, 17–35.

Neukum, G., et al. (2004b), Mars: Recent and episodic volcanic and glacial activity on Mars revealed by the High Resolution Stereo Camera, *Nature*, *432*, 971–979.

Oberbeck, V. R., W. L. Quade, and R. Greeley (1969), On the origin of lunar sinuous rilles, *Mod. Geol.*, *1*, 75–80.

Pickering, W. H. (1903), *The Moon*, pp. 42–43, Doubleday, New York.

Schubert, G., R. E. Lingenfelter, and S. J. Peale (1970), The morphology, distribution, and origin of lunar sinuous rilles, *Rev. Geophys.*, *8*, 199–225.

Shaw, H. R. (1972), Viscosities of magmatic silicate liquids: An empirical method of prediction, *Am. J. Sci.*, *272*, 870–893.

Squyres, S. W., et al. (2004), The Spirit rover's Athena science investigation at Gusev crater, Mars, *Science*, *305*, 794–799.

Walker, D., R. J. Kirkpatrick, J. Longhi, and J. F. Hays (1976), Crystallization history of lunar picritic basalt sample 12002: Phase-equilibria and cooling-rate studies, *Geol. Soc. Am. Bull.*, *87*, 646–656.

Williams, D. A., R. C. Kerr, and C. M. Lesher (1998), Emplacement and erosion by Archean komatiite lava flows at Kambalda: Revisited, *J. Geophys. Res.*, *103*, 27,533–27,550.

Williams, D. A., R. C. Kerr, and C. M. Lesher (1999), Thermal and fluid dynamics of komatiitic lavas associated with magmatic Ni-Cu- (PGE) sulphide deposits, in *Dynamic Processes in Magmatic Ore Deposits and Their Application in Mineral Exploration*, edited by R. R. Keays et al., *Geol. Assoc. Can. Short Course*, *13*, 367–412.

Williams, D. A., A. H. Wilson, and R. Greeley (2000a), A komatiite analog to potential ultramafic materials on Io, *J. Geophys. Res.*, *105*, 1671–1684.

Williams, D. A., S. A. Fagents, and R. Greeley (2000b), A reevaluation of the emplacement and erosional potential of turbulent, low-viscosity lavas on the Moon, *J. Geophys. Res.*, *105*, 20,189–20,206.

Williams, D. A., A. G. Davies, L. P. Keszthelyi, and R. Greeley (2001a), The July 1997 eruption at Pillan Patera on Io: Implications for ultrabasic lava flow emplacement, *J. Geophys. Res.*, *106*, 33,105–33,119.

Williams, D. A., R. Greeley, R. M. C. Lopes, and A. G. Davies (2001b), Evaluation of sulfur flow emplacement on Io from Galileo Data and numerical modeling, *J. Geophys. Res.*, *106*, 33,161–33,174.

Williams, D. A., R. C. Kerr, C. M. Lesher, and S. J. Barnes (2002), Analytical/numerical modeling of komatiite lava emplacement and thermal erosion at Perseverance, Western Australia, *J. Volcanol. Geotherm. Res.*, *110*(1–2), 27–55.

Williams, D. A., S. D. Kadel, R. Greeley, and C. M. Lesher (2004), Erosion by flowing lava: Geochemical evidence in the Cave Basalt, Mount St. Helens, Washington, *Bull. Volcanol.*, *66*(2), doi:10.1007/s00445-003-0301-2.

Wilson, A. H., and R. W. Carlson (1989), A Sm-Nd and Pb isotopic study of Archean greenstone belts in the southern Kaapvaal craton, South Africa, *Earth Planet. Sci. Lett.*, *96*, 89–105.

Wilson, L., and P. J. Mouginis-Mark (2001), Estimation of volcanic eruptions conditions for a large flank event on Elysium Mons, Mars, *J. Geophys. Res.*, *106*, 20,621–20,628.

R. Greeley and D. A. Williams, Department of Geological Sciences, Arizona State University, Box 871404, Tempe, AZ 85287-1404, USA. (david.williams@asu.edu)

K. Gwinner and E. Hauber, Deutsches Zentrum für Luft- und Raumfahrt, Berlin, Germany.

G. Neukum, Institute of Geological Sciences, Freie Universität, Berlin, Germany.